Development of innovative therapeutic strategies for osteoarthritis: exploring thermosensitive hydrogels, hiPSC-derived cells and cell-products, and novel drugs in preclinical models

Sayedipour, S.S.

Chapter 7

Appendix

A

Follow-up to Chapter 3

Spatial transcriptomics provides in-depth insight into the mode-of-action of hiPSC-derived stem cell treatment of human articular cartilage

*This chapter is included in the thesis booklet as an appendix and serves as a follow-up to **Chapter 3**, incorporating additional data from ex vivo human cartilage explants and mechanistic insights derived from spatial transcriptomics analyses (manuscript in preparation).*

Appendix Introduction: *ex vivo* and spatial transcriptomic follow-up studies of hiMSC+gel treatment

Building on the *in vivo* efficacy studies described in **Chapter 3**, this appendix presents additional *ex vivo* and spatial transcriptomic analyses aimed at further characterizing the effects of hiMSC-based therapy in a human-relevant context.

An *ex vivo* human osteoarthritic cartilage explant model was employed using tissue obtained from patients undergoing total joint replacement surgery. This model preserves the native extracellular matrix, cellular heterogeneity, and zonal organization of articular cartilage, thereby enabling direct assessment of treatment-induced changes within diseased human tissue. As such, it provides a complementary platform to the *in vivo* findings, allowing validation and extension of therapeutic effects observed in animal models.

In addition, spatial transcriptomic profiling was applied to treated and untreated lesioned human chondral explants to investigate the molecular mode of action of hiMSC therapy *in situ*. This approach enables high-resolution mapping of gene expression across distinct cartilage zones while maintaining spatial context, thereby capturing region-specific transcriptional responses that cannot be resolved using bulk analyses. Particular emphasis was placed on identifying consistent treatment-induced transcriptional alterations across donors and cartilage zones, with the aim of uncovering pathways associated with cartilage homeostasis, matrix remodeling, and inflammatory regulation.

Together, the *ex vivo* and spatial transcriptomic studies presented in this appendix serve to mechanistically contextualize the *in vivo* efficacy data reported in **chapter 3** in this thesis, strengthening the translational relevance of hiMSC-based therapeutic strategies for osteoarthritis.

Ex vivo Experimental design

To determine the direct effect of stem cells on cartilage, in the absence of interference of any additional factors such as synovium, a previously developed *ex vivo* explant model with knee joints included in the Research in Articular Osteoarthritis Cartilage (RAAK) study (1) was applied. **Figure 1** shows a schematic overview of the approach. In total, nine donors were included (characteristics shown in **Supplementary table S1**). Following generation of explants (8 mm diameter) they were allowed to equilibrate in serum-free medium for 72 h before the explants underwent a four-day treatment with hiMSCs+hydrogel. An advantage of the groove-model is that it is easier to apply the treatment locally, and cells+hydrogel remaining in place to a greater extent. Nonetheless, use of lesioned cartilage in the *ex vivo* model more authentically reflects degenerated OA cartilage. Therefore, we also assessed whether this could be applied to facilitate determination of the potential beneficial effects of stem cell treatments.

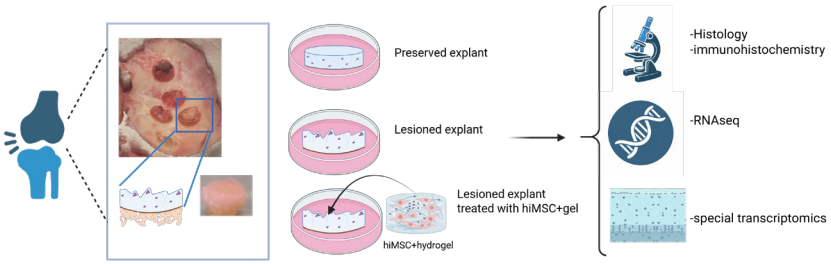

Figure 1. Schematic overview of the study (Created with Biorender.com)

Histological assessment *ex vivo* samples

For *ex vivo* analysis, cartilage explants were collected after treatment for both gene expression and histological evaluation. Samples were fixed in 4% paraformaldehyde, embedded in paraffin, and sectioned at 5 µm. Since the bone had been removed before the experiment, no decalcification step was required. Sections were stained with H&E or toluidine blue (TB) (Sigma-Aldrich) and mounted with Pertex (Sigma-Aldrich). Osteoarthritis-related cartilage damage was scored according to the Mankin grading system (2). In addition to the histological scoring, expression levels of relevant genes were determined by RT-qPCR and minus-ΔCt values were calculated using *GAPDH*, *SDHA* and *RPS11* as housekeeping genes.

RNA-sequencing

RNA sequencing analyses was performed on Controls (n=7 preserved, n=12 lesioned OA cartilage samples from N=9 donors) and Treated samples (n=17 lesioned OA cartilage samples treated with hiMSCs in the thermosensitive hydrogel from N=9 donors). Hereto, RNA was extracted with chloroform and purified using the RNeasy Mini Kit (QIAGEN). RNA libraries were generated (polyA enriched), and three-prime RNA sequencing was performed using Illumina NovaSeq 6000 according to the standard operating procedures based on the Illumina protocol for Paired-End Sequencing (PE150bp) with v1.5chemistry. Subsequently, the in-house available pipeline BioWDL (https://biowdl.github.io/RNA-seq/v5.0.0/index.html), developed by the Sequencing Analysis Support Core at Leiden University Medical Center, was used to process FASTQ files including adapter clipping with cutadapt.v2.10, and QC with FastQC.v0.11.9 and MultiQCv. 1.9. Furthermore, mapping was performed with STAR.v2.7.5a software and expression quantification and transcript assembly using HTSeq-Count.v.0.12.4. The reads were aligned to the human reference genome GRCh38 and Ensembl gene annotation version 109, and RNA-seq data was normalized using the DESeq2_v.1.30.0 R package. Before analysis, the data was transformed using the variance-stabilizing transforming (VST) method. Differential expression analysis was performed using the DESeq2 package v. 1.30.0 using R version 4.0.2. A general linear model (GLM), assuming a negative binomial distribution was applied, followed by a Wald-test to compare the control with treated explants. Benjamini-Hochberg multiple testing corrected P-values with a significance cut-off of 0.05 are reported as False Discovery Rate (FDR).

Spatial transcriptomics

Following RNAseq readout of the hiMSC treatment of lesioned OA cartilage explants, an optimal, tailored, probe panel was designed with the available online Xenium Panel Design Tool **(Supplementary table S2)** for genes to be detected at single cell level in their *in situ* geographic location (spatial transcriptomics). Spatial Transcriptomics was performed for two paired OA lesioned cartilage explants with or without hiMSC+hydrogel treatment. Target probes (N=295 genes) were selected with online available Xenium Panel Design Tool by means of being: Genes that are FDR significantly differentially expressed upon hiMSC+hydrogel treatment as determined by RNAseq (see also **Figure 2**); Notable genes that were FDR significantly differentially expressed with OA pathophysiology; and markers for cartilage damage were determined by the correlation of gene expression to Mankin scores. Genes that had extremely high expression levels in cartilage were excluded (e.g. *COL2A1* and *FN1*). With this we could compare changes upon treatment, also identify specific cell type or clusters with changes.

Spatial Transcriptomic analysis on 5 µm sections of paraffin-embedded cartilage explants (n=2 paired OA lesioned cartilage explants from *n*=2 donors) was performed by the Leiden Genome Technology Center (LGTC) using the 10X Genomics Xenium platform (v1) according to the manufacturer's protocol and initial data exploration was performed with online available Xenium Explorer 2.0.0 from 10X Genomics.

Statistical analysis

Statistical significance of average gene expression difference between controls and treated explants was estimated by the generalized estimating equation (GEE) with robust variance estimators for donor effects while adjusting for sex and age. Beta's were determined by the GEE during the modelling and represent the difference between the treated and control explants. *P*-values ≤ 0.05 were considered statistically significant. Differential expression analysis was performed in lesioned treated explants compared to non-treated lesioned explants using DESeq2 R package version 1.24. For protein-protein interactions, analysis was performed using the online tool STRING version 11.0 (3).

Results

Effects of stem cells treatment on cartilage integrity of lesioned human OA explants

Based on our *in vivo* findings we next aimed to study the effect of hiMSCs with hydrogel delivered in a human context using *ex vivo* cartilage explants obtained from OA patients. For simplicity, this treatment is referred to as hiMSC+gel. Prior to establishing the direct therapeutic efficacy of hiMSC+gel on human osteoarthritis articular cartilage, we selected a mRNA marker that could serve as a more sensitive proxy for structural articular cartilage damage. In doing so we analyzed human articular cartilage samples (*n*= 36 from 9 donors) of the RAAK-study for which both bulk mRNA sequencing and Mankin-scoring was assessed previously (4). Because of the strong and consistent

positive correlation that was observed between *TNFRSF11B* and Mankin-scores (FC = 0.81, $P = 8.6 \times 10^{-9}$, **Figure 2A**), the gene was prioritized as a marker of structural integrity of articular cartilage.

Next, the direct therapeutic efficacy was determined by comparing human lesioned OA articular cartilage with and without hiMSC+gel treatment, while preserved articular cartilage was used as reference.

As shown in **Figure 2B** hiMSC+gel treatment of lesioned articular cartilage samples reduced *TNFRSF11B* expression as marker of structural articular cartilage damage to that observed in preserved cartilage (**Figure 2C, 2D**). IHC revealed strong staining in the middle zone of lesioned cartilage, which was diminished upon treatment. Semi-quantitative blinded scoring supported these observations, showing significantly higher expression of TNFRSF11B in the middle zone of lesioned cartilage, with reduced expression after hiMSC+gel treatment.

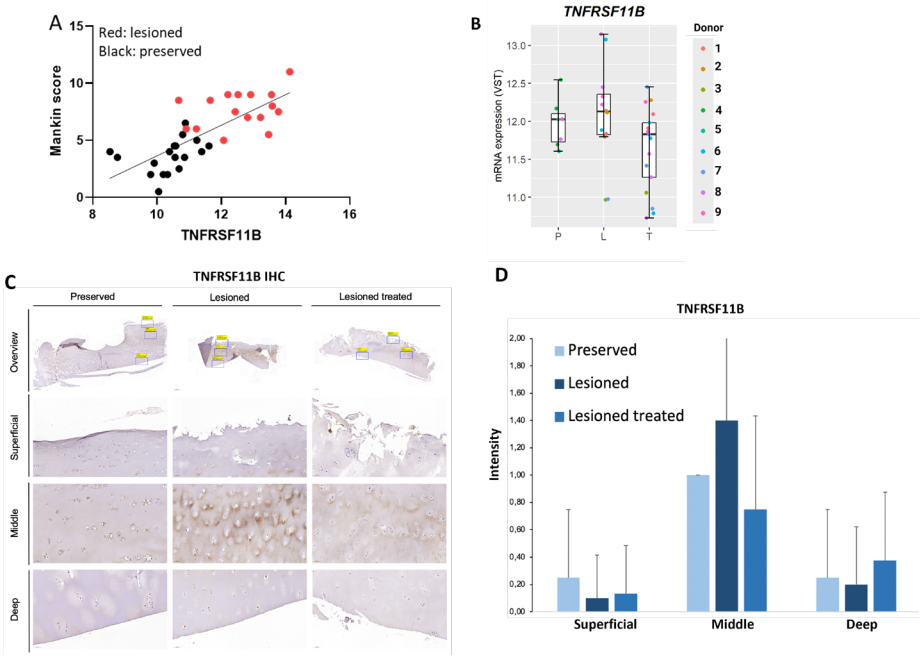

Figure 2. Potency of hiMSC+gel treatment to restore structural damage as measured by Mankin-score associated markers. (A) Correlation between Mankin score and *TNFRSF11B* (*P*=0.81 with *P*=8.6x10^{-9}) **(B)** Changes in *TNFRSF11B* gene expression in preserved, lesioned, and hiMSC+gel treated human *ex vivo* cartilage explants. **(C)** Immunohistochemistry for TNFRSF11B. Representative images for protein expression across the superficial, middle, and deep zone of articular cartilage as indicated. **(D)** Quantification of scoring for TNFRSF11B in Superficial, middle and deep zone of the cartilage.

To investigate the molecular effects of hiMSC+gel on human osteoarthritic chondrocytes, we next analyzed mRNA expression of key anabolic and catabolic markers in preserved, lesioned, and lesioned explants treated with hiMSC+gel (**Figure 3A**). Treatment with hiMSC+gel resulted in significant overall

upregulation of *COL2A1* expression (P = 3.87×10^{-2}) towards preserved tissue levels. In contrast, the catabolic metalloprotease *MMP13* showed only a modest non-significant reduction towards the preserved cartilage levels.

To gain further insight into transcriptome-wide processes marking hiMSC treatment, we performed bulk RNA sequencing of lesioned (untreated) and hiMSC+gel treated human cartilage explants. Differentially expressed gene (DEG) analysis revealed 28 significantly upregulated and 6 downregulated genes after treatment (FDR ≤ 0.05) **(Supplementary Table S3)**. The volcano plot (**Figure 3B**) indicated a particular upregulation of genes linked to sterol and fatty acid metabolism, including *MVD* (FC= 2.66, P= 2.09×10^{-09}), *MSMO1 (*FC= 2.82, P= 6.17×10^{-09}), *HMGCS1* (FC= 3.11, P= 8.23×10^{-09}), and *FABP3* (FC= 6.78, P= 8.77×10^{-09}) as also shown in the boxplots (**Figure 3C**).

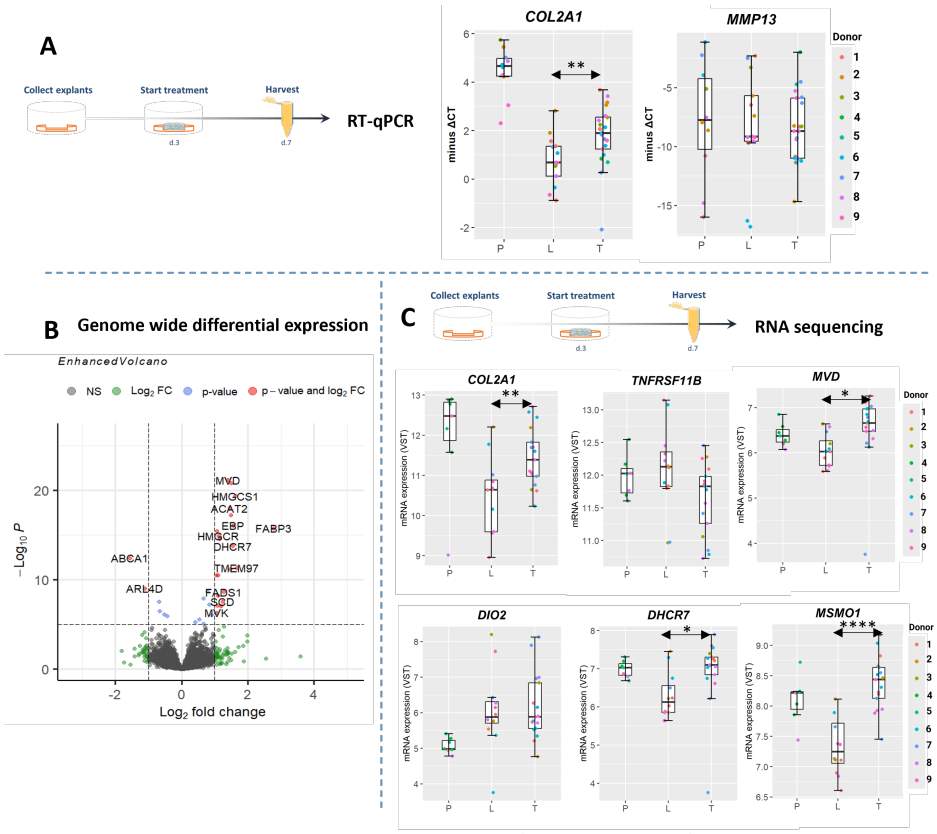

P= preserved, L= Lesioned, T= Treated (Lesioned+ hiMSC-gel)

Figure 3. Gene expression profiles in preserved, lesioned, and hiMSC-gel–treated cartilage explants. (A) RT-qPCR results for *COL2A1* and *MMP13*. **(B)** Volcano plot of differentially expressed genes from bulk RNA-seq comparing hiMSC-gel–treated and untreated lesioned cartilage. **(C)** Variance-stabilized transcript (VST) values for selected genes from RNA-seq. Boxplots show individual donor values, color-coded by donor ID. P= Preserved, L= Lesioned, T= Treated (Lesioned+hiMSC-gel) FC=fold change; FDR= false discovery rate; hiMSC= human-induced mesenchymal stem cell; VST= variance-stabilized transcript.

Spatial transcriptomics analysis

To investigate the mode of action of the hiMSC+gel treatment within native human cartilage, we performed spatial transcriptomics (Xenium, 10x genomics) with a custom probe panel of 295 genes (**Supplementary Table S2**). The panel included common cartilage and bone markers, as well as genes marking sterol and fatty acid metabolism identified by the bulk RNA sequencing. Spatial transcriptomics was performed on *n* = 7 control and hiMSC treated lesioned articular cartilage explants from two donors (**Figure 4**) of the RAAK study (donor 2: two treated and one untreated; donor 6: two treated and two untreated (**Figure 4A–B**) that enabled a robust *in situ* mapping of different cell clusters based on their transcriptome.

In total, 22.669 cells were detected. After quality control and filtering out cells with fewer than 10 transcripts 3.853 and 3.465 high quality cells from donor 2 and donor 6, respectively, remained for further analyses. To identify distinct cell populations based on the expression profile, we applied UMAP dimensionality reduction followed by Leiden clustering algorithm. UMAP analysis identified 10 transcriptionally distinct clusters (clusters 0–9) in donor 2 (**Figure 4A-2**) and nine clusters (0–8) in donor 6 (**Figure 4B-2**), indicating distinct cell populations within the lesioned cartilage. Mapping these clusters back to their *in situ* coordinates (**Figure 4A-3** and **Figure 4B-3**) revealed their spatial organization across the explants. Herein, distinct cell clusters could be recognized in the superficial zone (SZ), middle, and deep zone (DZ) of the untreated and/or treated lesioned explants, suggesting that hiMSC+gel treatment changed the transcriptional profile across chondrocyte zones. To distinguish molecular patterns of each cluster, differential expression (DE) between the chondrocyte populations was performed comparing each cluster against all others while selecting the top five most significant genes. As shown in **Figure 4A-4** and **Figure 4B-4**, these top five differentially expressed genes revealed distinct region-specific differential gene expression profiles. Herein, some genes were expressed in almost all cell clusters (e.g. *ACAN*) whereas some cell clusters had a very peculiar expression pattern marked by gene *DMP1* encoding dentin matrix acidic phosphoprotein 1 (cluster 9 in donor 2 and cluster 4 in donor 6), that is also known to mark osteocytes.

Treatment mode of action

Donor 2

Focusing on donor 2 (**Figure 5**), we observed distinct transcriptional alterations in the superficial zone (SZ) of treated cartilage explants compared with controls. In the SZ of the control explant, cluster 6 (dark pink) predominated, whereas in the treated explant, the SZ was dominated by cluster 8 (light green), suggesting that hiMSC-gel treatment reshaped the transcriptional landscape of cells in this region (**Figure 5A**). To explore these changes more deeply, we compared cluster 8 (treated SZ) with cluster 6 (control SZ). This analysis identified 116 FDR significant differentially expressed genes (DEGs) (**Supplementary Table S4**). Protein–protein interaction analysis (STRING) revealed highly interconnected networks among notable genes such as *ACAN*, *FRZB*, *MSMO1*, and *TNFRSF11B* (**Supplementary Figure S1A**).

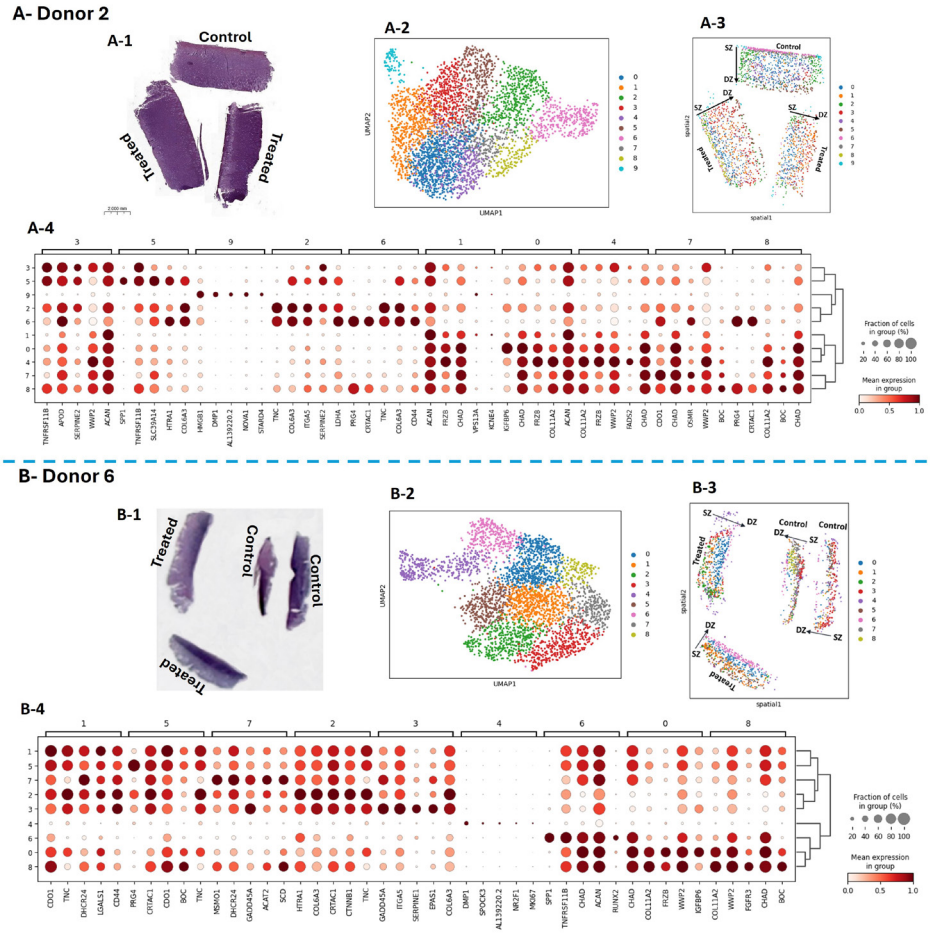

Figure 4. Spatial transcriptomic profiling of OA cartilage explants treated with hiMSC+gel. Spatial transcriptomics was performed on paired OA-lesioned cartilage explants from two donors (donor 2 and donor 6). **(A)** Representative explants from donor 2: **(A-1)** untreated control and hiMSC+gel-treated explants. **(A-2)** UMAP analysis identified 10 transcriptionally distinct clusters. **(A-3)** Clusters remapped to their spatial coordinates within the explant. **(A-4)** Dot plot showing differentially expressed genes (DEGs) across clusters. **(B)** Representative explants from donor 6: **(B-1)** untreated control and hiMSC+gel-treated explants. **(B-2)** UMAP analysis identified 9 transcriptionally distinct clusters. **(B-3)** Clusters remapped to their spatial coordinates within the explant. **(B-4)** Dot plot showing DEGs across clusters.

A

Differential gene expression analysis followed by Gene Ontology (GO) enrichment (**Figure 5B**) identified 38 upregulated and 77 downregulated genes (**Supplementary Table S4 a&b**). Upregulated genes were enriched in biological processes related to cartilage development, connective tissue development, Cholestesterol metabolic process. In contrast, downregulated genes were predominantly associated with leukocyte proliferation, ossification, and immune-related pathways. Gene-concept network analysis (**Figure 5C- Orange**) showed that the upregulated genes in the treated SZ were tightly associated with cartilage-specific and matrix-regulatory processes. Key genes included collagen alpha-2(XI) chain (*CHAD*) (FC= 37.6, FDR= 2.76 x 10^{-108}), *ACAN* (FC= 5.63, FDR= 3.57 x 10^{-92}), SRY-box Transcription Factor 9 (*SOX9)* (FC= 1.61, FDR= 9.94 x 10^{-4}), a transcriptional regulator essential for chondrocyte differentiation and activation of *COL2A1* expression; secreted frizzled-related protein 3 (*FRZB*) (FC= 9.28, FDR= 1.57 x 10^{-21}), and Chondroadherin-Like Protein (*CHADL)* (FC= 3.14, FDR= 1.91 x 10^{-2}), known to play a role in extracellular matrix organization. In addition, several genes involved in sterol and cholesterol biosynthesis were upregulated, including methylsterol monooxygenase 1 (*MSMO1*) (FC= 1.62, FDR= 4.88 x 10^{-2}), 7-dehydrocholesterol reductase (*DHCR7)* (FC= 2.43, FDR= 6,09 x 10^{-3}), enzymes central to sterol biosynthesis. These observations are in line with previous findings (**see Figure 3**), where *MSMO1* and *DHCR7* also showed reduced expression based on bulk RNA sequencing and VST counts. Conversely, downregulated genes (**Figure 5C- Green**) in Cluster 8 were enriched in immune-related pathways, including leukocyte proliferation, T-helper 17 (Th17) immune response, alpha-beta T cell differentiation, and responses to bacterial molecules such as lipopolysaccharide. The gene-concept network highlighted key genes such as Transforming Growth Factor Beta Receptor 1 *(TGFBR1)* (FC= 0.60, FDR= 1.16 x 10^{-2}), Tenascin C (*TNC*) (FC =0.17, FDR= 3.27 x 10^{-47}), *MMP13* (FC=0.01, P= 1.36×10^{-3}), *ADAMTS5* (FC= 0.13, FDR= 6,49 x 10^{-5}), Insulin-like Growth Factor Binding Protein 3 *(IGFBP3) (*FC= 2.34×10^{-8}, P= 1.79 × 10^{-4}), *DIO2* (FC= 0.15, FDR=8.68 x 10^{-11}), and Serpin Family E Member 1 (*SERPINE1*)(FC= 0.21, FDR= 1.84 x 10^{-7}*),* all of which showed reduced expression following treatment.

Donor 6

To validate the robustness of our previous observations, we performed a spatial transcriptomic analysis in a second donor (donor 6). Similar to donor 2, we observed a clear zonal pattern of cell clusters extending from the SZ to the DZ. Focusing again on the SZ, we specifically compared Cluster 1 in the treated explant with Cluster 3 in the untreated (control) explant. (**Figure 6A**). Differential gene expression analysis between Cluster 1 and Cluster 3 identified 129 genes with significant FDR changes, comprising 28 upregulated and 95 downregulated transcripts (**Supplementary Table S5 a&b**). STRING protein–protein interaction network analysis showed that these DGEs formed a highly interconnected network centered on extracellular matrix (ECM) and cartilage-related genes (*FRZB*, *ACAN*, *SOX9*) (**Supplementary Figure S1B**). Gene Ontology enrichment further demonstrated that upregulated genes were significantly associated with cartilage development, connective tissue organization, skeletal system morphogenesis, and chondrocyte differentiation, while downregulated genes were enriched in immune-related pathways, negative regulation of catalytic activity, and regulation of neurogenesis (**Figure 6B)**. Upregulated genes involved in regenerative pathways included *CHAD* (FC=

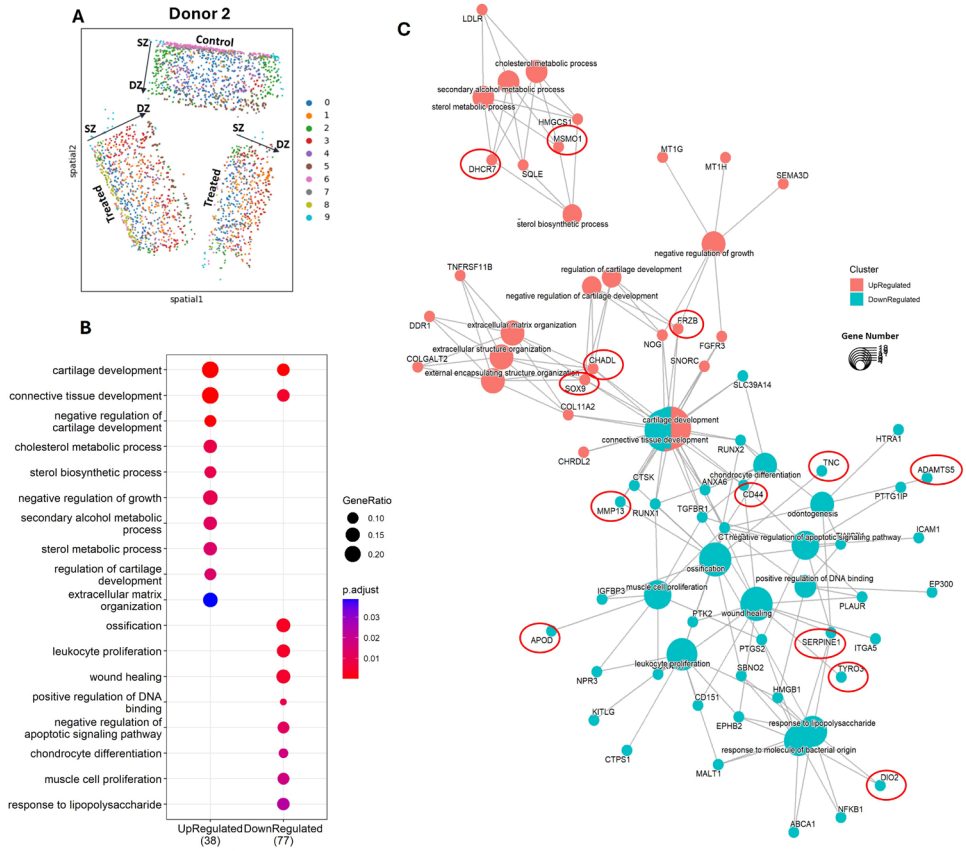

Figure 5. Spatial transcriptomic comparison between control and hiMSC-treated cartilage explants from donor 2.

(A) Spatial clustering of gene expression in control and treated explants, with clusters annotated across the SZ and DZ. **(B)** GO enrichment analysis of differentially expressed genes in Donor 2, Cluster 8 (treated) versus Cluster 6 (control), showing upregulated and downregulated biological processes. **(C)** Gene network of upregulated and downregulated genes genes in Cluster 8 versus Cluster 6, with selected genes highlighted. SZ: superficial zone; DZ: deep zone; GO: Gene Ontology; hiMSC: human induced mesenchymal stromal cell.

A

17.4, FDR= 2.15 x 10^{-155}), *ACAN* (FC= 1.63, FDR=2.19 x 10^{-29}), *SOX5* (FC= 1.51, FDR= 4.55 x 10^{-7}), *SOX9* (FC= 1.46, FDR= 9.33 x 10^{-5}), *CHADL* (FC= 11.27, FDR=1.24 x 10^{-12}), *FRZB* (FC= 8.56, FDR= 1.30 x 10^{-17}) (**Figure 6C- Orange**), supporting the activation of a cartilage-specific gene program following hiMSC+gel treatment. These findings are consistent with the transcriptional profile observed in donor 2 (**Figure 5**). Conversely, downregulated genes (**Figure 6C- Green**) such as complement Decay-Accelerating Factor (*CD55)* (FC= 0.36, FDR= 4.18 x 10^{-23}), *SERPINE1* (FC= 0.19, FDR=1.04×10^{-48}),

Osteopontin (*SPP1*) (FC= 0.11, FDR= 7.17 x 10^{-7}), and nerve growth factor *(NGF*)(FC= 0.31, FDR= 3.83 x 10^{-4}), were among the most suppressed in the treated samples related to regulation of neurogenesis and immune-related pathways.

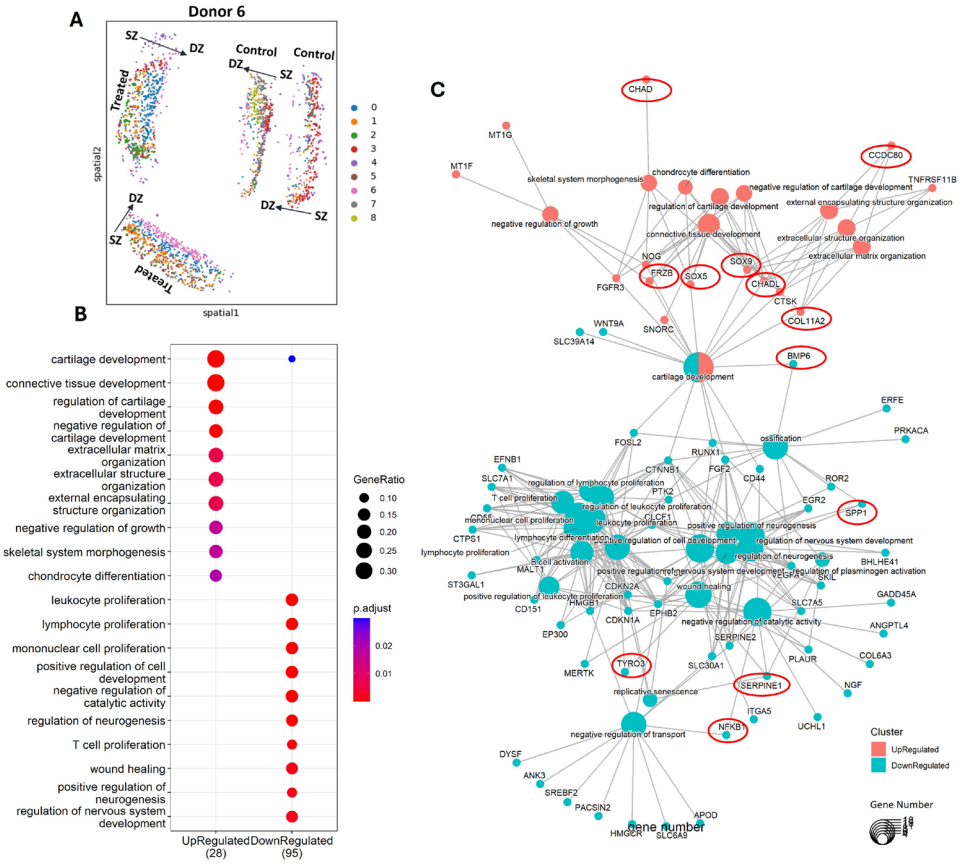

Figure 6. Spatial transcriptomic comparison between control and hiMSC-treated cartilage explants from donor 6. (A) Spatial clustering of gene expression in control and treated explants, with clusters annotated across the SZ and DZ. **(B)** GO enrichment analysis of differentially expressed genes in Cluster 1 (treated) versus Cluster 3 (control), showing upregulated and downregulated biological processes. **(C)** Gene network of upregulated and down regulated genes in Cluster 1 versus Cluster 3, with selected genes highlighted. SZ: superficial zone; DZ: deep zone; GO: Gene Ontology; hiMSC: human induced mesenchymal stromal cell.

To evaluate the consistency of gene expression changes between the two donors (donor 2-cluster 8 vs 6 and donor 6-cluster 1 vs 3), we compared their lists of significantly upregulated and downregulated genes using Venn diagrams, shown in **Figure 7**.

For upregulated genes (**Figure 7A**), we observed 15 genes were commonly upregulated in both donors. This corresponds to approximately 39.5% of the upregulated genes in donor 2 (8 vs 6) and 54% in donor 6 (1 vs 3), indicating a moderate overlap in the transcriptional response between donors. Notable shared genes include *CHAD*, *ACAN*, *FRZB*, and *SOX9*, all of which are known to play critical roles in cartilage homeostasis and extracellular matrix production. The STRING protein-protein interaction network for these shared upregulated genes reveals a tightly connected cluster involving ECM-associated genes and key transcription factors such as *SOX9*, suggesting a coordinated anabolic response. Similarly, comparison of downregulated genes (**Figure 7B**) showed a high degree of overlap, with 43 genes commonly downregulated across both donors. This accounts for 55% of downregulated genes in donor 2 (8 vs 6) and 43% in donor 6 (1 vs 3). Shared downregulated genes include *SERPINE1*, *CD44*, *SLC30A1*, *TYRO3*, and *APOD*, many of which are involved in inflammation, lipid metabolism, and cell adhesion. The corresponding STRING network highlights complex interconnectivity among these genes.

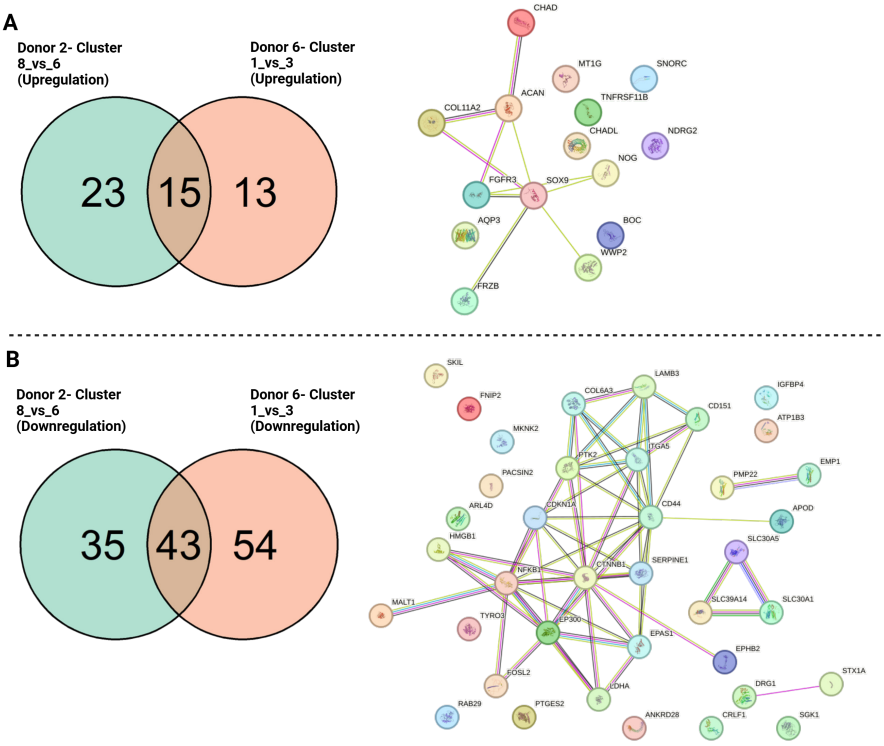

Figure 7 Comparison of differentially expressed genes between donors 2 and 6. (A) Venn diagram showing overlap of upregulated genes between donor 2- cluster 8 vs 6 and donor 6- cluster 1 vs 3 with STRING network illustrating protein–protein interactions among the 18 commonly upregulated genes.**(B)** Venn diagram showing overlap of downregulated genes between donor 2- cluster 8 vs 6 and donor 6- cluster 1 vs 3 with STRING network illustrating protein–protein interactions among the 43 commonly downregulated genes.

Discussion

In this study, we evaluated the therapeutic effects of hiMSCs in osteoarthritis using a stepwise approach that combined *in vivo* and *ex vivo* models with spatial transcriptomic analyses. hiMSCs delivered via an optimized thermosensitive hydrogel consistently demonstrated chondroprotective effects, reflected by reduced cartilage damage and enhanced anabolic responses. Beyond confirming their therapeutic benefit, our findings highlight both structural and metabolic mechanisms underlying hiMSC-mediated cartilage repair, including modulation of extracellular matrix organization, lipid metabolism, and inflammatory pathways.

In our study, we employed both an *in vivo* DMM mouse model (**Chapter 3**) and a human *ex vivo* explant model of lesioned OA cartilage to evaluate the therapeutic efficacy of hiMSCs. The preclinical animal model has the advantage that the entire synovial compartment is included, thereby allowing inflammatory processes to be taken along in disease progression (5). It also enabled us to test the effect of recently developed thermosensitive hydrogel for intra-articular injections in a controlled joint environment (6, 7) However, murine OA pathophysiology is not identical to that of humans, and animal studies inherently conflict with the principles of the 3Rs (Replacement, Reduction, Refinement) (8). By contrast, the human explant model provides a faithful representation of human OA cartilage, as we specifically used lesioned tissue directly obtained from patients (9). Despite the heterogeneity that characterizes OA in humans, we observed significant treatment effects across explants, indicating the robustness of the approach. Since in our setup we kept explants for one week in culture, matrix-level changes could not be fully assessed; instead, we used molecular markers as biomarker of cartilage damage. Bulk RNA sequencing identified *TNFRSF11B* as a key damage-associated gene, consistent with earlier reports (10), and immunohistochemistry confirmed its strong expression in lesioned regions, establishing it as a treatment-responsive marker that complements the matrix-level insights from the animal model.

In our human *ex vivo* cartilage explant study bulk mRNA sequencing was used as sensitive readout of the molecular phenotypic changes of the human chondrocyte in the overall cartilage tissue in response to hiMSC treatment. Despite donor heterogeneity, the analysis consistently revealed upregulation of genes involved in cholesterol biosynthesis and lipid regulatory networks, pathways critical for chondrocyte function, extracellular matrix (ECM) synthesis, and cartilage maintenance (9). Notably, genes such as *MVD*, *DHCR7*, *MSMO1*, and *FABP3* have been implicated in promoting cartilage homeostasis and protecting against osteoarthritic degeneration. Genes like *DHCR7* and *MSMO1* encode enzymes that influence chondrocyte metabolism (9). DHCR7 is essential for converting 7-dehydrocholesterol to cholesterol, a step critical for proper primary cilium formation and Hedgehog signaling. Since primary cilia act as important sensory organelles in chondrocytes, regulating responses to mechanical and biochemical signals that maintain cartilage homeostasis (11, 12). Upregulation of *DHCR7* in the hiMSC-gel treatment group may therefore support restoration of cholesterol biosynthesis, enhance ciliary function, and promote anabolic signaling, ultimately contributing to cartilage repair. Similarly, *MSMO1* encodes methyl sterol monooxygenase 1, an enzyme involved in the demethylation of sterol intermediates during cholesterol biosynthesis. This step is essential for proper chondrocyte differentiation, growth plate formation and endochondral ossification (13). Upregulation of *MSMO1* in the treated cartilage likely reflects activation of sterol

biosynthesis pathways, consistent with a metabolically restorative response that supports chondrocyte survival and ECM production (14). Moreover, the targeted mRNA expression levels of *COL2A1* appeared to be significantly upregulated restored in hiMSC treated samples, confirming restoration of anabolic activation in treated chondrocytes of our DMM mouse model. However, although some reduction in *MMP13* was observed it did not reach statistical significance.

Spatial transcriptomic analysis provided a unique opportunity to map the molecular effects of hiMSC-gel treatment within the native architecture of osteoarthritic cartilage. The analysis was performed on $n = 7$ lesioned cartilage explants from two independent donors, allowing direct pairwise comparison between treated and untreated samples from the same donor. Using a tailored probe panel of 295 genes derived from the bulk transcriptomic dataset representing pathways involved in cartilage homeostasis, degeneration, and repair, we visualized how treatment modulated chondrocyte states *in situ*. This approach revealed distinct, zone-specific transcriptional responses that were not apparent in bulk RNA sequencing, indicating the spatial heterogeneity of chondrocyte activity across cartilage zones. Consistent with the bulk RNA-seq data, genes associated with cholesterol and lipid biosynthesis, including *MSMO1* and *DHCR7*, were strongly upregulated in the superficial zone of treated explants, confirming the robustness of the observed metabolic reprogramming.

Beyond confirming these metabolic signatures, spatial analysis provided higher sensitivity for detecting localized anabolic responses and zone-restricted transcriptional changes. Notably, hiMSC-gel treatment induced a robust upregulation of *SOX9* and its downstream targets specifically within the superficial zone, a region typically depleted of anabolic activity in OA cartilage (15). Importantly, *SOX9* expression was not evident in the bulk RNA-seq dataset but was clearly detected in the spatial analysis, underscoring the advantage of this technology in revealing localized regenerative responses that remain masked in bulk transcriptomic profiling. *SOX9* is a regulator of chondrogenesis, essential for the activation of *COL2A1* and the maintenance of chondrocyte phenotype promote chondrocyte proliferation, and inhibit chondrocyte apoptosis (16-18). Another upregulated gene upon hiMSC+gel treatment was *FRZB,* an antagonist of Wnt signaling, is known to protect cartilage by inhibiting hypertrophic differentiation and osteophyte formation (19). *CHADL* is involved in extracellular matrix (ECM) organization and collagen binding, supporting proper cartilage architecture and is a negative modulator of chondrocyte differentiation (20). Upregulation of these genes collectively points to activation of reparative and anti-hypertrophic pathways in treated cartilage.

To further explore the therapeutic action across the cartilage depth, zone-resolved analyses revealed that hiMSC treatment reprogrammed the superficial zone by upregulating key regulators of cartilage development while downregulating mediators of inflammation, matrix degradation, and neurogenic signaling. *MMP13*, a collagenase responsible for degrading type II collagen, is a well-established driver of cartilage destruction in OA. Its downregulation indicates reduced catabolic activity. *TGFBR1*, although generally involved in tissue homeostasis, has been associated with pathological TGF-β signaling in OA, promoting fibrosis and osteophyte formation; its suppression may therefore reflect normalization of aberrant signaling (21). Additionally, TGF-β1 plays a key role in MSC chondrogenic differentiation, particularly in synergy with vitamin D, which promotes MSC proliferation and migration. This interaction is mediated through regulation of the ERK/JNK signaling pathway, highlighting a complex but coordinated control of cartilage repair processes (22). *CD55*, while typically

anti-inflammatory, is paradoxically elevated in OA and may contribute to dysregulated immune responses in the joint (23). Its downregulation suggests modulation of complement activity toward a more balanced immune environment. Finally, suppression of *SPP1*, also known as osteopontin, a cytokine-like protein involved in bone remodeling, ECM breakdown, and macrophage recruitment (24), along with *NGF*, suggests a reduction in inflammatory signaling, tissue breakdown, and nociceptive pathway activation commonly associated with OA pathology. *NGF* which supports the survival and differentiation of sensory neurons and plays a central role in pain signaling, was similarly reduced. In OA, elevated *NGF* levels are strongly associated with pain sensitization and neurogenic inflammation (25). Moreover, *NGF* promotes immune cell recruitment and angiogenesis within the joint, further contributing to disease progression. Suppression of *NGF* expression following treatment could therefore reduce joint pain, inhibit aberrant nerve growth in cartilage, and attenuate neuroinflammation, key therapeutic targets in OA pain management.

In conclusion, our work demonstrates that intra-articular delivery of hiMSCs using a thermosensitive hydrogel confers robust chondroprotective effects in *in vivo* and *ex vivo* models of osteoarthritis. Beyond structural preservation and anabolic support, the treatment induced metabolic and spatially defined transcriptional changes that provide new mechanistic insights into cartilage regeneration. These findings establish hiMSC-hydrogel therapy as a promising strategy for OA and underscore the importance of integrating multi-level analyses to guide the development of effective regenerative treatments.

Funding

The research leading to these results has received funding from the European Union's Horizon 2020 research and innovation program AutoCRAT under grant agreement No 874671. The material presented and views expressed here are the responsibility of the author(s) only. The EU Commission takes no responsibility for any use made of the information set out.

Patient consent for publication

Not applicable.

Ethics approval

The Medical Ethics Committee of the LUMC gave approval for generation of hiPSCs from skin fibroblasts of healthy donors under number P13.080 on July 2 2014 (Parapluprotocol: hiPSC). Informed consent was obtained from all donors.

Collection of hBMSCs from OA patients undergoing total joint replacement surgery is approved by the Medical Ethical Committee of the LUMC within the ongoing RAAK study and available under numbers P08.239 and P19.013.

References

1. Ramos YF, den Hollander W, Bovee JV, Bomer N, van der Breggen R, Lakenberg N, et al. Genes involved in the osteoarthritis process identified through genome wide expression analysis in articular cartilage; the RAAK study. PloS one. 2014;9(7):e103056.

2. Mankin HJ, Dorfman H, Lippiello L, Zarins A. Biochemical and metabolic abnormalities in articular cartilage from osteo-arthritic human hips: II. Correlation of morphology with biochemical and metabolic data. JBJS. 1971;53(3):523–37.

3. Szklarczyk D, Gable AL, Lyon D, Junge A, Wyder S, Huerta-Cepas J, et al. STRING v11: protein–protein association networks with increased coverage, supporting functional discovery in genome-wide experimental datasets. Nucleic acids research. 2019;47(D1):D607–D13.

4. Dambrot C, Van De Pas S, Van Zijl L, Brändl B, Wang J, Schalij M, et al. Polycistronic lentivirus induced pluripotent stem cells from skin biopsies after long term storage, blood outgrowth endothelial cells and cells from milk teeth. Differentiation. 2013;85(3):101–9.

5. Glasson S, Blanchet T, Morris E. The surgical destabilization of the medial meniscus (DMM) model of osteoarthritis in the 129/SvEv mouse. Osteoarthritis and cartilage. 2007;15(9):1061–9.

6. Sayedipour SS, Schomann T, van de Looij SM, Rezaie S, Ramos YF, Vermonden T, et al. Advancing Therapeutic Solutions: Poloxamer-based Thermosensitive Injectable Hydrogels containing a Self-assembling Peptide for In situ Gelation in an Osteoarthritis Murine Model. bioRxiv. 2025:2025.04. 30.651282.

7. Sayedipour SS, Schomann T, van de Looij SM, Rezaie S, Ramos YF, Vermonden T, et al. Poloxamer-based Thermosensitive Injectable Hydrogels containing a Self-assembling Peptide for In situ Gelation. Computational and Structural Biotechnology Journal. 2025.

8. Russell WMS, Burch RL, Hume CW. The principles of humane experimental technique: Methuen London; 1959.

9. Houtman E, Tuerlings M, Suchiman HED, Lakenberg N, Cornelis FM, Mei H, et al. Inhibiting thyroid activation in aged human explants prevents mechanical induced detrimental signalling by mitigating metabolic processes. Rheumatology. 2023;62(1):457–66.

10. Rodríguez Ruiz A, Tuerlings M, Das A, Coutinho de Almeida R, Suchiman HED, Nelissen RG, et al. The role of TNFRSF11B in development of osteoarthritic cartilage. Rheumatology. 2022;61(2):856–64.

11. Suzuki A, Ogata K, Yoshioka H, Shim J, Wassif CA, Porter FD, et al. Disruption of Dhcr7 and Insig1/2 in cholesterol metabolism causes defects in bone formation and homeostasis through primary cilium formation. Bone research. 2020;8(1):1.

12. Ali SA, Al-Jazrawe M, Ma H, Whetstone H, Poon R, Farr S, et al. Regulation of cholesterol homeostasis by hedgehog signaling in osteoarthritic cartilage. Arthritis & Rheumatology. 2016;68(1):127–37.

13. Anderson RA, Schwalbach KT, Mui SR, LeClair EE, Topczewska JM, Topczewski J. Zebrafish models of skeletal dysplasia induced by cholesterol biosynthesis deficiency. Disease models & mechanisms. 2020;13(6):dmm042549.

14. Su Z, Zong Z, Deng J, Huang J, Liu G, Wei B, et al. Lipid metabolism in cartilage development, degeneration, and regeneration. Nutrients. 2022;14(19):3984.

15. Govindaraj K, Kannan S, Coutinho de Almeida R, Jansen Klomp L, Karperien M, Meulenbelt I, et al. Dissecting SOX9 dynamics reveals its differential regulation in osteoarthritis. Journal of cellular physiology. 2024;239(12):e31443.

16. ter Huurne M, Schelbergen R, Blattes R, Blom A, de Munter W, Grevers LC, et al. Antiinflammatory and chondroprotective effects of intraarticular injection of adipose-derived stem cells in experimental osteoarthritis. Arthritis & Rheumatism. 2012;64(11):3604–13.

17. Wang S, Lei B, Zhang E, Gong P, Gu J, He L, et al. Targeted therapy for inflammatory diseases with mesenchymal stem cells and their derived exosomes: from basic to clinics. International Journal of Nanomedicine. 2022:1757–81.

18. Lefebvre V, Behringer R, De Crombrugghe B. L-Sox5, Sox6 and Sox9 control essential steps of the chondrocyte differentiation pathway. Osteoarthritis and cartilage. 2001;9:S69–S75.

19. Enomoto-Iwamoto M, Kitagaki J, Koyama E, Tamamura Y, Wu C, Kanatani N, et al. The Wnt antagonist Frzb-1 regulates chondrocyte maturation and long bone development during limb skeletogenesis. Developmental biology. 2002;251(1):142–56.

20. Tuerlings M, van Hoolwerff M, Houtman E, Suchiman EH, Lakenberg N, Mei H, et al. RNA sequencing reveals interacting key determinants of osteoarthritis acting in subchondral bone and articular cartilage: identification of IL11 and CHADL as attractive treatment targets. Arthritis & Rheumatology. 2021;73(5):789–99.

21. Xu X, Zheng L, Yuan Q, Zhen G, Crane JL, Zhou X, et al. Transforming growth factor-β in stem cells and tissue homeostasis. Bone research. 2018;6(1):2.

22. Jiang X, Huang B, Yang H, Li G, Zhang C, Yang G, et al. TGF-β1 is involved in vitamin D-induced chondrogenic differentiation of bone marrow-derived mesenchymal stem cells by regulating the ERK/JNK pathway. Cellular Physiology and Biochemistry. 2017;42(6):2230–41.

23. Silawal S, Triebel J, Bertsch T, Schulze-Tanzil G. Osteoarthritis and the complement cascade. Clinical Medicine Insights: Arthritis and Musculoskeletal Disorders. 2018;11:1179544117751430.

24. Martín-Márquez BT, Sandoval-García F, Corona-Meraz FI, Martínez-García EA, Sánchez-Hernández PE, Salazar-Páramo M, et al. Osteopontin: a bone-derived protein involved in rheumatoid arthritis and osteoarthritis immunopathology. Biomolecules. 2023;13(3):502.

25. Schmelz M, Mantyh P, Malfait A-M, Farrar J, Yaksh T, Tive L, et al. Nerve growth factor antibody for the treatment of osteoarthritis pain and chronic low-back pain: mechanism of action in the context of efficacy and safety. Pain. 2019;160(10):2210–20.

Supplementary Figures

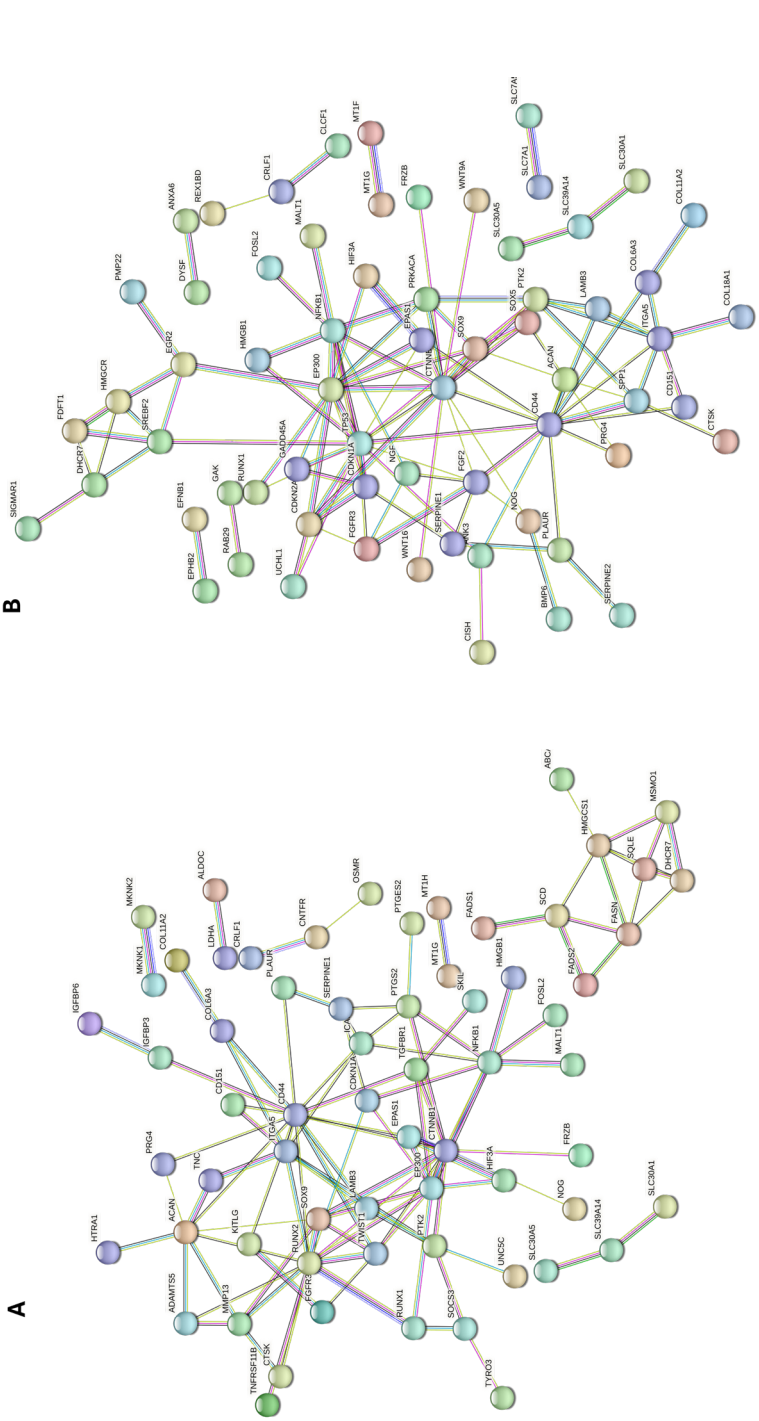

Supplementary Figure S1. STRING protein–protein interaction network of significantly differentially expressed genes (DEGs) in the superficial zone of hiMSC+gel–treated explants compared to untreated explants in (A) Donor 2 and **(B) Donor 6.** Link thickness indicates the strength of evidence supporting the interaction. Required interaction score= High confidence (0.700).

Supplementary Tables

Supplementary Table S1. Donor characteristics

Donor	Sex	Age
1	F	83
2	M	72
3	F	78
4	F	66
5	F	72
6	F	78
7	M	62
8	M	68
9	F	74

F= Female, M= Male.

Supplementary Table S2. Genes included in the Xenium probe panel for spatial transcriptomic analysis

	Gene name	Ensembl gene ID		Gene name	Ensembl gene ID
1	*ABCA1*	ENSG00000165029	**25**	*BHLHE41*	ENSG00000123095
2	*ACAN*	ENSG00000157766	**26**	*BLVRB*	ENSG00000090013
3	*ACAT2*	ENSG00000120437	**27**	*BMP6*	ENSG00000153162
4	*ACSS2*	ENSG00000131069	**28**	*BMPR1B*	ENSG00000138696
5	*ADAMTS5*	ENSG00000154736	**29**	*BOC*	ENSG00000144857
6	*ADAMTS6*	ENSG00000049192	**30**	*CCDC80*	ENSG00000091986
7	*ADGRV1*	ENSG00000164199	**31**	*CCL18*	ENSG00000275385
8	*ADRM1*	ENSG00000130706	**32**	*CCL2*	ENSG00000108691
9	*ALDH1A2*	ENSG00000128918	**33**	*CD151*	ENSG00000177697
10	*ALDOC*	ENSG00000109107	**34**	*CD44*	ENSG00000026508
11	*ALPK2*	ENSG00000198796	**35**	*CD55*	ENSG00000196352
12	*ALPL*	ENSG00000162551	**36**	*CDKN1A*	ENSG00000124762
13	*AMD1*	ENSG00000123505	**37**	*CDKN2A*	ENSG00000147889
14	*ANGPTL4*	ENSG00000167772	**38**	*CDO1*	ENSG00000129596
15	*ANK3*	ENSG00000151150	**39**	*CHAD*	ENSG00000136457
16	*ANKRD28*	ENSG00000206560	**40**	*CHADL*	ENSG00000100399
17	*ANOS1*	ENSG00000011201	**41**	*CHD9*	ENSG00000177200
18	*ANXA6*	ENSG00000197043	**42**	*CH1*	ENSG00000134121
19	*AOC2*	ENSG00000131480	**43**	*CHRDL2*	ENSG00000054938
20	*APOD*	ENSG00000189058	**44**	*CHST3*	ENSG00000122863
21	*AQP3*	ENSG00000165272	**45**	*CISH*	ENSG00000114737
22	*ARL4D*	ENSG00000175906	**46**	*CLCF1*	ENSG00000175505
23	*ATP1B3*	ENSG00000069849	**47**	*CLIC3*	ENSG00000169583
24	*BDNF*	ENSG00000176697	**48**	*CNTFR*	ENSG00000122756

[Continued next page]

Supplementary Table S2. *[Continued]*

	Gene name	Ensembl gene ID		Gene name	Ensembl gene ID
49	*CNTN2*	ENSG00000184144	**94**	*FDPS*	ENSG00000160752
50	*COL10A1*	ENSG00000123500	**95**	*FGF2*	ENSG00000138685
51	*COL11A2*	ENSG00000204248	**96**	*FGFR3*	ENSG00000068078
52	*COL22A1*	ENSG00000169436	**97**	*FNIP2*	ENSG00000052795
53	*COL5A1*	ENSG00000130635	**98**	*FOSL2*	ENSG00000075426
54	*COL6A3*	ENSG00000163359	**99**	*FRZB*	ENSG00000162998
55	*COLGALT2*	ENSG00000198756	**100**	*GADD45A*	ENSG00000116717
56	*CRLF1*	ENSG00000006016	**101**	*GAK*	ENSG00000178950
57	*CRTAC1*	ENSG00000095713	**102**	*GDF5*	ENSG00000125965
58	*CSF1R*	ENSG00000182578	**103**	*GDF7*	ENSG00000143869
59	*CTNNB1*	ENSG00000168036	**104**	*GLIS3*	ENSG00000107249
60	*CTPS1*	ENSG00000171793	**105**	*GRIA2*	ENSG00000120251
61	*CTSK*	ENSG00000143387	**106**	*GRIK3*	ENSG00000163873
62	*CXCL14*	ENSG00000145824	**107**	*GRIK5*	ENSG00000105737
63	*CXCL8*	ENSG00000169429	**108**	*HCFC1R1*	ENSG00000103145
64	*DCC*	ENSG00000187323	**109**	*HELLS*	ENSG00000119969
65	*DDR1*	ENSG00000204580	**110**	*HIF3A*	ENSG00000124440
66	*DHCR24*	ENSG00000116133	**111**	*HMGB1*	ENSG00000189403
67	*DHCR7*	ENSG00000172893	**112**	*HMGCR*	ENSG00000113161
68	*DIO2*	ENSG00000211448	**113**	*HMGCS1*	ENSG00000112972
69	*DMP1*	ENSG00000152592	**114**	*HSD11B2*	ENSG00000176387
70	*DNER*	ENSG00000187957	**115**	*HSD17B7*	ENSG00000132196
71	*DRG1*	ENSG00000185721	**116**	*HSPA2*	ENSG00000126803
72	*DRG2*	ENSG00000108591	**117**	*HSPB6*	ENSG00000004776
73	*DRGX*	ENSG00000165606	**118**	*HTRA1*	ENSG00000166033
74	*DUSP5*	ENSG00000138166	**119**	*HYAL1*	ENSG00000114378
75	*DYSF*	ENSG00000135636	**120**	*ICAM1*	ENSG00000090339
76	*EBP*	ENSG00000147155	**121**	*IDI1*	ENSG00000067064
77	*EFNB1*	ENSG00000090776	**122**	*IGFBP1*	ENSG00000146678
78	*EFNB3*	ENSG00000108947	**123**	*IGFBP3*	ENSG00000146674
79	*EGR2*	ENSG00000122877	**124**	*IGFBP4*	ENSG00000141753
80	*ELOVL6*	ENSG00000170522	**125**	*IGFBP6*	ENSG00000167779
81	*EMP1*	ENSG00000134531	**126**	*IL10*	ENSG00000136634
82	*ENSG00000230615*	ENSG00000230615	**127**	*IL11*	ENSG00000095752
83	*EP300*	ENSG00000100393	**128**	*IL6*	ENSG00000136244
84	*EPAS1*	ENSG00000116016	**129**	*IP6K2*	ENSG00000068745
85	*EPHB2*	ENSG00000133216	**130**	*ISM2*	ENSG00000100593
86	*EPHB4*	ENSG00000196411	**131**	*ITGA5*	ENSG00000161638
87	*ERFE*	ENSG00000178752	**132**	*KCNE4*	ENSG00000152049
88	*ERG28*	ENSG00000133935	**133**	*KDM7A*	ENSG00000006459
89	*FABP3*	ENSG00000121769	**134**	*KIF1A*	ENSG00000130294
90	*FADS1*	ENSG00000149485	**135**	*KITLG*	ENSG00000049130
91	*FADS2*	ENSG00000134824	**136**	*LAMB3*	ENSG00000196878
92	*FASN*	ENSG00000169710	**137**	*LDHA*	ENSG00000134333
93	*FDFT1*	ENSG00000079459	**138**	*LDLR*	ENSG00000130164

[Continued next page]

Supplementary Table S2. *[Continued]*

	Gene name	Ensembl gene ID		Gene name	Ensembl gene ID
139	*LGALS1*	ENSG00000100097	**183**	*ORMDL2*	ENSG00000123353
140	*LGR5*	ENSG00000139292	**184**	*OSMR*	ENSG00000145623
141	*LIF*	ENSG00000128342	**185**	*P3H2*	ENSG00000090530
142	*LMNB1*	ENSG00000113368	**186**	*PACSIN2*	ENSG00000100266
143	*LRRC1*	ENSG00000137269	**187**	*PAPPA*	ENSG00000182752
144	*LSS*	ENSG00000160285	**188**	*PCDHB7*	ENSG00000113212
145	*LTK*	ENSG00000062524	**189**	*PCYT2*	ENSG00000185813
146	*MALT1*	ENSG00000172175	**190**	*PDIA5*	ENSG00000065485
147	*MDGA1*	ENSG00000112139	**191**	*PLAUR*	ENSG00000011422
148	*MEPE*	ENSG00000152595	**192**	*PLOD2*	ENSG00000152952
149	*MERTK*	ENSG00000153208	**193**	*PLXND1*	ENSG00000004399
150	*MKI67*	ENSG00000148773	**194**	*PMP22*	ENSG00000109099
151	*MKNK1*	ENSG00000079277	**195**	*POSTN*	ENSG00000133110
152	*MKNK2*	ENSG00000099875	**196**	*PPP1R14C*	ENSG00000198729
153	*MMAB*	ENSG00000139428	**197**	*PRG4*	ENSG00000116690
154	*MMP13*	ENSG00000137745	**198**	*PRKACA*	ENSG00000072062
155	*MSMO1*	ENSG00000052802	**199**	*PRKCA*	ENSG00000154229
156	*MT1F*	ENSG00000198417	**200**	*PRRG4*	ENSG00000135378
157	*MT1G*	ENSG00000125144	**201**	*PTGES*	ENSG00000148344
158	*MT1H*	ENSG00000205358	**202**	*PTGES2*	ENSG00000148334
159	*MUC1*	ENSG00000185499	**203**	*PTGS2*	ENSG00000073756
160	*MVD*	ENSG00000167508	**204**	*PTK2*	ENSG00000169398
161	*MVK*	ENSG00000110921	**205**	*PTPRD*	ENSG00000153707
162	*MYO10*	ENSG00000145555	**206**	*PTPRD-AS1*	ENSG00000225706
163	*N4BP3*	ENSG00000145911	**207**	*PTPRE*	ENSG00000132334
164	*NCKIPSD*	ENSG00000213672	**208**	*PTTG1IP*	ENSG00000183255
165	*NDNF*	ENSG00000173376	**209**	*PXYLP1*	ENSG00000155893
166	*NDRG2*	ENSG00000165795	**210**	*R3HDML*	ENSG00000101074
167	*NELL1*	ENSG00000165973	**211**	*RAB29*	ENSG00000117280
168	*NETO1*	ENSG00000166342	**212**	*RALGAPA2*	ENSG00000188559
169	*NFKB1*	ENSG00000109320	**213**	*RAPGEF2*	ENSG00000109756
170	*NGF*	ENSG00000134259	**214**	*RCAN2*	ENSG00000172348
171	*NKX2-2*	ENSG00000125820	**215**	*RDH11*	ENSG00000072042
172	*NOG*	ENSG00000183691	**216**	*RELN*	ENSG00000189056
173	*NOVA1*	ENSG00000139910	**217**	*REX1BD*	ENSG00000006015
174	*NPR3*	ENSG00000113389	**218**	*RIPK4*	ENSG00000183421
175	*NPTX2*	ENSG00000106236	**219**	*RNF152*	ENSG00000176641
176	*NR2F1*	ENSG00000175745	**220**	*ROR2*	ENSG00000169071
177	*NR2F2*	ENSG00000185551	**221**	*RUNX1*	ENSG00000159216
178	*NRP1*	ENSG00000099250	**222**	*RUNX2*	ENSG00000124813
179	*NRP2*	ENSG00000118257	**223**	*S100A2*	ENSG00000196754
180	*NSDHL*	ENSG00000147383	**224**	*SBNO2*	ENSG00000064932
181	*NTF3*	ENSG00000185652	**225**	*SC5D*	ENSG00000109929
182	*NTRK3*	ENSG00000140538	**226**	*SCD*	ENSG00000099194

[Continued next page]

Supplementary Table S2. *[Continued]*

	Gene name	Ensembl gene ID		Gene name	Ensembl gene ID
227	*SEC61A1*	ENSG00000058262	**257**	*SQLE*	ENSG00000104549
228	*SEMA3D*	ENSG00000153993	**258**	*SREBF2*	ENSG00000198911
229	*SERPINE1*	ENSG00000106366	**259**	*ST3GAL1*	ENSG00000008513
230	*SERPINE2*	ENSG00000135919	**260**	*ST6GALNAC5*	ENSG00000117069
231	*SF3A2*	ENSG00000104897	**261**	*STAB1*	ENSG00000010327
232	*SGK1*	ENSG00000118515	**262**	*STARD4*	ENSG00000164211
233	*SIGMAR1*	ENSG00000147955	**263**	*STMN2*	ENSG00000104435
234	*SIRT1*	ENSG00000096717	**264**	*STX1A*	ENSG00000106089
235	*SKIL*	ENSG00000136603	**265**	*TFPI2*	ENSG00000105825
236	*SLC20A1*	ENSG00000144136	**266**	*TGFA*	ENSG00000163235
237	*SLC25A1*	ENSG00000100075	**267**	*TGFBR1*	ENSG00000106799
238	*SLC29A2*	ENSG00000174669	**268**	*THRB*	ENSG00000151090
239	*SLC30A1*	ENSG00000170385	**269**	*TIMELESS*	ENSG00000111602
240	*SLC30A5*	ENSG00000145740	**270**	*TMEM176A*	ENSG00000002933
241	*SLC39A14*	ENSG00000104635	**271**	*TMEM255B*	ENSG00000184497
242	*SLC6A1*	ENSG00000157103	**272**	*TMEM59L*	ENSG00000105696
243	*SLC6A2*	ENSG00000103546	**273**	*TMEM97*	ENSG00000109084
235	*SKIL*	ENSG00000136603	**274**	*TMPRSS4*	ENSG00000137648
236	*SLC20A1*	ENSG00000144136	**275**	*TNC*	ENSG00000041982
237	*SLC25A1*	ENSG00000100075	**276**	*TNFRSF11B*	ENSG00000164761
238	*SLC29A2*	ENSG00000174669	**277**	*TNR*	ENSG00000116147
239	*SLC30A1*	ENSG00000170385	**278**	*TP53*	ENSG00000141510
240	*SLC30A5*	ENSG00000145740	**279**	*TPP1*	ENSG00000166340
241	*SLC39A14*	ENSG00000104635	**280**	*TRIB2*	ENSG00000071575
242	*SLC6A1*	ENSG00000157103	**281**	*TRPV1*	ENSG00000196689
243	*SLC6A2*	ENSG00000103546	**282**	*TSC1*	ENSG00000165699
244	*SLC6A9*	ENSG00000196517	**283**	*TSPAN2*	ENSG00000134198
245	*SLC7A1*	ENSG00000139514	**284**	*TWIST1*	ENSG00000122691
246	*SLC7A5*	ENSG00000103257	**285**	*TYRO3*	ENSG00000092445
247	*SLC9B2*	ENSG00000164038	**286**	*UCHL1*	ENSG00000154277
248	*SNCG*	ENSG00000173267	**287**	*UNC5C*	ENSG00000182168
249	*SNORC*	ENSG00000182600	**288**	*VEGFA*	ENSG00000112715
250	*SOCS3*	ENSG00000184557	**289**	*VPS13A*	ENSG00000197969
251	*SOX10*	ENSG00000100146	**290**	*WNT10B*	ENSG00000169884
252	*SOX5*	ENSG00000134532	**291**	*WNT16*	ENSG00000002745
253	*SOX6*	ENSG00000110693	**292**	*WNT9A*	ENSG00000143816
254	*SOX9*	ENSG00000125398	**293**	*WWP2*	ENSG00000198373
255	*SPOCK3*	ENSG00000196104	**294**	*ZBTB21*	ENSG00000173276
256	*SPP1*	ENSG00000118785	**295**	*ZNF778*	ENSG00000170100

Supplementary Table S3. Investigation of the FDR significant genes in Bulk RNA sequencing of lesioned treated with hiMSC-gel with lesioned untreated control

	Gene	FC	*P*-value	FDR*
		Up-regulated		
1	*MVD*	2.66	2.09×10^{-9}	2.74×10^{-5}
2	*MSMO1*	2.82	6.17×10^{-9}	2.88×10^{-5}
3	*HMGCS1*	3.11	8.23×10^{-9}	2.88×10^{-5}
4	*FABP3*	6.78	8.77×10^{-9}	2.88×10^{-5}
5	*ACAT2*	2.76	1.37×10^{-8}	3.59×10^{-5}
6	*EBP*	2.95	1.98×10^{-8}	4.34×10^{-5}
7	*FDPS*	2.8	2.87×10^{-8}	5.39×10^{-5}
8	*FDFT1*	2.1	6.01×10^{-8}	9.72×10^{-5}
9	*SQLE*	2.23	6.66×10^{-8}	9.72×10^{-5}
10	*HMGCR*	2.19	7.50×10^{-8}	9.86×10^{-5}
11	*DHCR7*	2.9	1.93×10^{-7}	2.11×10^{-4}
12	*TMEM97*	3.1	4.78×10^{-7}	4.83×10^{-4}
13	*LDLR*	2.73	9.21×10^{-7}	8.25×10^{-4}
14	*IDI1*	2.15	1.00×10^{-6}	8.25×10^{-4}
15	*ERG28*	2.07	1.01×10^{-6}	8.25×10^{-4}
16	*PCYT2*	1.72	3.34×10^{-6}	2.58×10^{-3}
17	*MMAB*	2.14	4.43×10^{-6}	3.06×10^{-3}
18	*ALDOC*	1.57	7.82×10^{-6}	4.67×10^{-3}
19	*FADS1*	2.4	1.00×10^{-5}	5.69×10^{-3}
20	*LSS*	1.79	1.06×10^{-5}	5.69×10^{-3}
21	*ACSS2*	2.3	1.18×10^{-5}	5.96×10^{-3}
22	*SCD*	2.36	2.49×10^{-5}	1.21×10^{-2}
23	*FADS2*	2.11	2.96×10^{-5}	1.36×10^{-2}
24	*MVK*	2.11	3.00×10^{-5}	1.36×10^{-2}
25	*PTPRD.AS1*	1.64	5.03×10^{-5}	2.20×10^{-2}
26	*NSDHL*	1.88	6.83×10^{-5}	2.89×10^{-2}
27	*SREBF2*	1.44	8.52×10^{-5}	3.49×10^{-2}
28	*DHCR24*	1.59	1.24×10^{-4}	4.77×10^{-2}
		Down-regulated		
1	*ABCA1*	-2.93	1.01×10^{-7}	1.21×10^{-4}
2	*KDM7A*	-1.61	4.43×10^{-6}	3.06×10^{-3}
3	*ARL4D*	-2.14	4.97×10^{-6}	3.27×10^{-3}
4	*TRIB2*	-1.6	7.14×10^{-6}	4.46×10^{-3}
5	*MYO10*	-1.43	1.08×10^{-5}	5.69×10^{-3}
6	*ATP1B3*	-1.36	1.18×10^{-4}	4.69×10^{-2}

*To correct for multiple testing. the Benjamini–Hochberg method was applied to *P*-values and reported as the FDR. Gene expression changes measured in RNA sequencing data between lesioned OA articular cartilage treated with hiMSC-gel and lesioned OA articular cartilage untreated as reference. FC: fold change; FDR: false discovery rate

Supplementary Table S4. Chanes in gene expression in special transcriptomics profile upon hiMSC+gel treatment of in Donor 2- cluster 8 vs 6.

Supplementary Table S4. (a) Upregulated DEGs- Donor 2- Cluster 8 vs 6

	Gene	FC	*P*-value	FDR*
1	*CHAD*	37.64	9.60×10^{-111}	2.76×10^{-108}
2	*ACAN*	5.63	2.49×10^{-94}	3.57×10^{-92}
3	*COL11A2*	10.29	2.61×10^{-55}	1.87×10^{-53}
4	*WWP2*	4.40	2.48×10^{-43}	1.02×10^{-41}
5	*TNFRSF11B*	3.63	3.80×10^{-25}	1.09×10^{-23}
6	*FRZB*	9.28	6.57×10^{-23}	1.57×10^{-21}
7	*FGFR3*	6.50	4.30×10^{-14}	5.87×10^{-13}
8	*SNORC*	5.54	3.11×10^{-14}	4.46×10^{-13}
9	*BOC*	3.72	9.33×10^{-12}	9.91×10^{-11}
10	*IGFBP6*	4.60	3.60×10^{-11}	3.69×10^{-10}
11	*CHRDL2*	36.58	4.65×10^{-8}	4.30×10^{-7}
12	*FADS2*	4.48	1.67×10^{-6}	1.30×10^{-5}
13	*NDRG2*	2.56	1.06×10^{-5}	6.94×10^{-5}
14	*P3H2*	12.49	7.53×10^{-5}	4.00×10^{-4}
15	*CXCL14*	38.80	1.00×10^{-4}	5.04×10^{-4}
16	*SQLE*	2.56	8.72×10^{-5}	4.55×10^{-4}
17	*FADS1*	2.39	1.17×10^{-4}	5.79×10^{-4}
18	*ALDOC*	2.38	1.87×10^{-4}	8.26×10^{-4}
19	*FASN*	2.94	2.09×10^{-4}	9.07×10^{-4}
20	*SOX9*	1.61	2.32×10^{-4}	9.94×10^{-4}
21	*SLC6A9*	5.92	2.78×10^{-4}	1.14×10^{-3}
22	*MT1H*	2.39	3.68×10^{-4}	1.49×10^{-3}
23	*COLGALT2*	2.85	8.07×10^{-4}	3.09×10^{-3}
24	*MT1G*	2.06	8.45×10^{-4}	3.19×10^{-3}
25	*HMGCS1*	2.10	1.75×10^{-3}	6.09×10^{-3}
26	*DHCR7*	2.43	1.76×10^{-3}	6.09×10^{-3}
27	*RCAN2*	3.78	2.07×10^{-3}	7.06×10^{-3}
28	*CNTFR*	20.84	2.24×10^{-3}	7.58×10^{-3}
29	*UNC5C*	4.13	3.58×10^{-3}	1.16×10^{-2}
30	*CHADL*	3.14	6.38×10^{-3}	1.91×10^{-2}
31	*NOG*	9.09	7.45×10^{-3}	2.16×10^{-2}
32	*SCD*	1.76	7.44×10^{-3}	2.16×10^{-2}
33	*LDLR*	3.09	8.36×10^{-3}	2.35×10^{-2}
34	*CHST3*	1.50	8.84×10^{-3}	2.46×10^{-2}
35	*SEMA3D*	3.57	1.19×10^{-2}	3.13×10^{-2}
36	*DDR1*	3.25	1.88×10^{-2}	4.72×10^{-2}
37	*AQP3*	3.01	1.97×10^{-2}	4.88×10^{-2}
38	*MSMO1*	1.62	1.97×10^{-2}	4.88×10^{-2}

Supplementary Table S4. (b) (partial) Downregulated DEGs- for Donor 2- Cluster 8 vs 6

	Gene	FC	*P*-value	FDR*
1	*SLC30A1*	0.60	1.84×10^{-2}	4.67×10^{-2}
2	*RUNX2*	0.00	1.59×10^{-2}	4.08×10^{-2}
3	*CTSK*	0.64	1.43×10^{-2}	3.70×10^{-2}
4	*OSMR*	0.76	1.29×10^{-2}	3.37×10^{-2}
5	*PTGES2*	0.46	1.10×10^{-2}	2.91×10^{-2}
6	*KITLG*	0.34	1.08×10^{-2}	2.91×10^{-2}
7	*MKNK2*	0.50	1.01×10^{-2}	2.73×10^{-2}
8	*SLC9B2*	0.48	9.28×10^{-3}	2.54×10^{-2}
9	*EPHB2*	0.11	9.12×10^{-3}	2.52×10^{-2}
10	*PTK2*	0.61	8.34×10^{-3}	2.35×10^{-2}
11	*PTGS2*	0.00	8.03×10^{-3}	2.30×10^{-2}
12	*CTPS1*	0.36	7.04×10^{-3}	2.08×10^{-2}
13	*GLIS3*	0.24	5.77×10^{-3}	1.74×10^{-2}
14	*ATP1B3*	0.62	5.23×10^{-3}	1.60×10^{-2}
15	*TYRO3*	0.39	4.94×10^{-3}	1.52×10^{-2}
16	*SPOCK3*	0.08	4.34×10^{-3}	1.35×10^{-2}
17	*ANGPTL4*	0.17	4.18×10^{-3}	1.32×10^{-2}
18	*ABCA1*	0.39	3.83×10^{-3}	1.22×10^{-2}
19	*PACSIN2*	0.61	3.59×10^{-3}	1.16×10^{-2}
20	*TGFBR1*	0.60	3.53×10^{-3}	1.16×10^{-2}
21	*LGALS1*	0.64	2.95×10^{-3}	9.83×10^{-3}
22	*NPR3*	0.00	1.65×10^{-3}	5.85×10^{-3}
23	*SF3A2*	0.57	1.54×10^{-3}	5.53×10^{-3}
24	*CD151*	0.71	1.39×10^{-3}	5.07×10^{-3}
25	*MMP13*	0.00	1.36×10^{-3}	5.01×10^{-3}
26	*IP6K2*	0.46	1.16×10^{-3}	4.34×10^{-3}
27	*HIF3A*	0.46	6.35×10^{-4}	2.46×10^{-3}
28	*MALT1*	0.31	4.64×10^{-4}	1.82×10^{-3}
29	*PLAUR*	0.34	4.40×10^{-4}	1.76×10^{-3}
30	*FOSL2*	0.50	2.60×10^{-4}	1.08×10^{-3}
31	*DRG1*	0.48	2.43×10^{-4}	1.03×10^{-3}
32	*SLC39A14*	0.73	1.75×10^{-4}	7.99×10^{-4}
33	*IGFBP3*	0.00	1.79×10^{-4}	8.01×10^{-4}
34	*ICAM1*	0.42	1.67×10^{-4}	7.75×10^{-4}
35	*CHD9*	0.45	1.66×10^{-4}	7.75×10^{-4}
36	*NFKB1*	0.43	1.48×10^{-4}	7.06×10^{-4}
37	*SLC30A5*	0.42	1.31×10^{-4}	6.38×10^{-4}
38	*RUNX1*	0.51	9.22×10^{-5}	4.73×10^{-4}
39	*PTTG1IP*	0.64	7.34×10^{-5}	3.97×10^{-4}
40	*DRG2*	0.31	5.91×10^{-5}	3.26×10^{-4}
41	*SKIL*	0.41	3.35×10^{-5}	1.88×10^{-4}
42	*SOCS3*	0.29	1.84×10^{-5}	1.06×10^{-4}
43	*SGK1*	0.32	1.83×10^{-5}	1.06×10^{-4}

[Continued next page]

Supplementary Table S4. (b) (partial) *[Continued]*

	Gene	FC	*P*-value	FDR*
44	*CDO1*	0.69	1.49×10^{-5}	8.92×10^{-5}
45	*EPAS1*	0.54	1.46×10^{-5}	8.92×10^{-5}
46	*MKNK1*	0.18	1.17×10^{-5}	7.31×10^{-5}
47	*EP300*	0.38	1.10×10^{-5}	6.99×10^{-5}
48	*ADAMTS5*	0.13	9.72×10^{-6}	6.49×10^{-5}
49	*ANXA6*	0.50	7.13×10^{-6}	4.87×10^{-5}
50	*STX1A*	0.12	4.65×10^{-6}	3.25×10^{-5}
51	*LAMB3*	0.09	2.69×10^{-6}	1.93×10^{-5}
52	*FNIP2*	0.30	2.02×10^{-6}	1.49×10^{-5}
53	*RALGAPA2*	0.17	1.79×10^{-6}	1.35×10^{-5}
54	*CDKN1A*	0.35	4.91×10^{-7}	3.91×10^{-6}
55	*ARL4D*	0.23	3.10×10^{-7}	2.54×10^{-6}
56	*TWIST1*	0.00	2.60×10^{-7}	2.19×10^{-6}
57	*SBNO2*	0.48	1.37×10^{-7}	1.19×10^{-6}
58	*PTPRE*	0.25	5.82×10^{-8}	5.22×10^{-7}
59	*SERPINE1*	0.21	1.92×10^{-8}	1.84×10^{-7}
60	*ITGA5*	0.54	8.49×10^{-10}	8.40×10^{-9}
61	*CRLF1*	0.15	7.87×10^{-12}	8.68×10^{-11}
62	*DIO2*	0.15	5.34×10^{-12}	6.13×10^{-11}
63	*IGFBP4*	0.05	4.42×10^{-12}	5.28×10^{-11}
64	*HMGB1*	0.36	8.51×10^{-13}	1.06×10^{-11}
65	*RAB29*	0.16	1.90×10^{-13}	2.48×10^{-12}
66	*CD44*	0.45	1.70×10^{-14}	2.56×10^{-13}
67	*PRG4*	0.61	9.85×10^{-15}	1.57×10^{-13}
68	*CTNNB1*	0.44	2.82×10^{-15}	4.77×10^{-14}
69	*MYO10*	0.13	1.10×10^{-15}	1.98×10^{-14}
70	*ANKRD28*	0.15	1.05×10^{-17}	2.15×10^{-16}
71	*CRTAC1*	0.45	1.13×10^{-17}	2.15×10^{-16}
72	*PMP22*	0.37	1.44×10^{-18}	3.18×10^{-17}
73	*APOD*	0.44	5.82×10^{-24}	1.52×10^{-22}
74	*LDHA*	0.36	4.75×10^{-27}	1.51×10^{-25}
75	*EMP1*	0.19	3.07×10^{-34}	1.10×10^{-32}
76	*TNC*	0.17	6.83×10^{-49}	3.27×10^{-47}
77	*HTRA1*	0.15	7.37×10^{-53}	4.23×10^{-51}

*To correct for multiple testing. the Benjamini–Hochberg method was applied to *P*-values and reported as the FDR. Gene expression changes measured in RNA sequencing data between lesioned OA articular cartilage treated with hiMSC-gel and lesioned OA articular cartilage untreated as reference. FC: fold change; FDR: false discovery rate

Supplementary Table S5. Chanes in gene expression in special transcriptomics profile upon hiMSC+gel treatment of in Donor 6- cluster 1 vs 3.

Supplementary Table S5. (a) Upregulated DEGs- Donor 6- Cluster 1 vs 3

	Gene	FC	*P*-value	FDR*
1	*CHAD*	17.46	7.33×10^{-158}	2.15×10^{-155}
2	*PRG4*	8.79	7.41×10^{-125}	1.09×10^{-122}
3	*WWP2*	2.90	3.36×10^{-39}	1.65×10^{-37}
4	*ACAN*	1.63	5.96×10^{-31}	2.19×10^{-29}
5	*CDO1*	2.11	8.84×10^{-26}	2.00×10^{-24}
6	*FRZB*	8.56	7.51×10^{-19}	1.30×10^{-17}
7	*TNFRSF11B*	2.32	6.86×10^{-19}	1.26×10^{-17}
8	*COL11A2*	2.71	7.37×10^{-15}	9.85×10^{-14}
9	*NDRG2*	3.51	1.87×10^{-14}	2.30×10^{-13}
10	*CHADL*	11.27	1.09×10^{-13}	1.24×10^{-12}
11	*FGFR3*	4.13	1.34×10^{-13}	1.45×10^{-12}
12	*BOC*	2.25	1.58×10^{-13}	1.66×10^{-12}
13	*MT1F*	2.41	4.50×10^{-8}	3.23×10^{-7}
14	*SOX5*	1.51	6.65×10^{-8}	4.55×10^{-7}
15	*HSPB6*	2.18	6.53×10^{-7}	4.00×10^{-6}
16	*CTSK*	1.72	8.69×10^{-7}	5.01×10^{-6}
17	*AQP3*	3.27	1.42×10^{-6}	7.75×10^{-6}
18	*CCDC80*	1.50	6.69×10^{-6}	3.17×10^{-5}
19	*SNORC*	1.86	8.48×10^{-6}	3.90×10^{-5}
20	*SOX9*	1.46	2.10×10^{-5}	9.33×10^{-5}
21	*GRIK3*	4.06	3.78×10^{-5}	1.64×10^{-4}
22	*MT1G*	1.41	3.58×10^{-3}	1.12×10^{-2}
23	*CLIC3*	2.88	3.97×10^{-3}	1.20×10^{-2}
24	*NOG*	5.18	4.42×10^{-3}	1.30×10^{-2}
25	*WNT16*	14.86	9.61×10^{-3}	2.48×10^{-2}
26	*ADGRV1*	2.57	1.12×10^{-2}	2.80×10^{-2}
27	*HIF3A*	1.53	1.17×10^{-2}	2.88×10^{-2}
28	*NPR3*	2.21	1.89×10^{-2}	4.44×10^{-2}

Supplementary Table S5. (b) Downregulated DEGs- Donor 6- Cluster1 vs 3

	Gene	FC	*P*-value	FDR*
1	*WNT9A*	0.10	2.08×10^{-2}	4.84×10^{-2}
2	*CDKN2A*	0.39	1.85×10^{-2}	4.38×10^{-2}
3	*FDFT1*	0.81	1.52×10^{-2}	3.63×10^{-2}
4	*FNIP2*	0.71	1.39×10^{-2}	3.35×10^{-2}
5	*EFNB1*	0.41	1.33×10^{-2}	3.24×10^{-2}
6	*REX1BD*	0.49	1.32×10^{-2}	3.24×10^{-2}
7	*FADS1*	0.76	1.13×10^{-2}	2.80×10^{-2}
8	*HMGCR*	0.67	1.06×10^{-2}	2.68×10^{-2}
9	*KDM7A*	0.63	1.00×10^{-2}	2.56×10^{-2}
10	*EGR2*	0.00	7.89×10^{-3}	2.05×10^{-2}

[Continued next page]

Supplementary Table S5. (b) (partial) *[Continued]*

	Gene	FC	*P*-value	FDR*
11	*RNF152*	0.60	7.34×10^{-3}	1.93×10^{-2}
12	*CISH*	0.26	6.90×10^{-3}	1.83×10^{-2}
13	*DUSP5*	0.16	6.84×10^{-3}	1.83×10^{-2}
14	*MALT1*	0.66	6.14×10^{-3}	1.66×10^{-2}
15	*PTGES2*	0.58	6.09×10^{-3}	1.66×10^{-2}
16	*PTK2*	0.74	5.98×10^{-3}	1.64×10^{-2}
17	*EP300*	0.70	5.80×10^{-3}	1.61×10^{-2}
18	*SLC30A1*	0.68	5.60×10^{-3}	1.57×10^{-2}
19	*VPS13A*	0.59	5.26×10^{-3}	1.49×10^{-2}
20	*RUNX1*	0.71	4.95×10^{-3}	1.41×10^{-2}
21	*ANGPTL4*	0.28	4.85×10^{-3}	1.40×10^{-2}
22	*ANXA6*	0.77	4.59×10^{-3}	1.33×10^{-2}
23	*CTPS1*	0.45	4.42×10^{-3}	1.30×10^{-2}
24	*PLAUR*	0.59	4.31×10^{-3}	1.29×10^{-2}
25	*ERFE*	0.52	3.75×10^{-3}	1.15×10^{-2}
26	*APOD*	0.84	3.74×10^{-3}	1.15×10^{-2}
27	*GAK*	0.67	3.52×10^{-3}	1.11×10^{-2}
28	*PTPRE*	0.64	3.16×10^{-3}	1.01×10^{-2}
29	*DYSF*	0.33	2.92×10^{-3}	9.42×10^{-3}
30	*RAB29*	0.66	2.71×10^{-3}	8.84×10^{-3}
31	*PRKACA*	0.72	2.17×10^{-3}	7.24×10^{-3}
32	*DHCR7*	0.64	1.81×10^{-3}	6.12×10^{-3}
33	*SREBF2*	0.77	1.52×10^{-3}	5.20×10^{-3}
34	*ORMDL2*	0.51	1.43×10^{-3}	4.96×10^{-3}
35	*ST3GAL1*	0.67	1.33×10^{-3}	4.64×10^{-3}
36	*EPHB2*	0.13	1.12×10^{-3}	3.96×10^{-3}
37	*BHLHE41*	0.68	9.21×10^{-4}	3.30×10^{-3}
38	*SLC30A5*	0.60	6.44×10^{-4}	2.34×10^{-3}
39	*TYRO3*	0.53	5.05×10^{-4}	1.86×10^{-3}
40	*ROR2*	0.51	3.81×10^{-4}	1.42×10^{-3}
41	*SIGMAR1*	0.56	3.63×10^{-4}	1.37×10^{-3}
42	*ANKRD28*	0.69	3.50×10^{-4}	1.35×10^{-3}
43	*CLCF1*	0.30	3.53×10^{-4}	1.35×10^{-3}
44	*IGFBP6*	0.66	9.69×10^{-5}	3.83×10^{-4}
45	*NGF*	0.31	9.76×10^{-5}	3.83×10^{-4}
46	*ANK3*	0.68	7.61×10^{-5}	3.07×10^{-4}
47	*ZBTB21*	0.52	4.87×10^{-5}	1.99×10^{-4}
48	*MERTK*	0.32	4.32×10^{-5}	1.79×10^{-4}
49	*NCKIPSD*	0.51	4.09×10^{-5}	1.72×10^{-4}
50	*UCHL1*	0.28	3.99×10^{-5}	1.70×10^{-4}
51	*SLC7A5*	0.61	2.62×10^{-5}	1.15×10^{-4}
52	*BMP6*	0.25	9.55×10^{-6}	4.32×10^{-5}
53	*PPP1R14C*	0.45	6.98×10^{-6}	3.26×10^{-5}
54	*SERPINE2*	0.68	6.12×10^{-6}	2.95×10^{-5}

[Continued next page]

Supplementary Table S5. (b) (partial) *[Continued]*

	Gene	FC	*P*-value	FDR*
55	*SLC6A9*	0.42	5.00×10^{-6}	2.45×10^{-5}
56	*NFKB1*	0.51	3.99×10^{-6}	1.99×10^{-5}
57	*ATP1B3*	0.63	3.52×10^{-6}	1.78×10^{-5}
58	*TP53*	0.58	3.04×10^{-6}	1.57×10^{-5}
59	*FOSL2*	0.51	2.20×10^{-6}	1.15×10^{-5}
60	*PACSIN2*	0.63	1.70×10^{-6}	9.07×10^{-6}
61	*AMD1*	0.40	1.42×10^{-6}	7.75×10^{-6}
62	*SLC39A14*	0.70	9.13×10^{-7}	5.16×10^{-6}
63	*SKIL*	0.54	7.74×10^{-7}	4.55×10^{-6}
64	*TPP1*	0.64	7.35×10^{-7}	4.41×10^{-6}
65	*PMP22*	0.71	4.50×10^{-7}	2.82×10^{-6}
66	*ADRM1*	0.55	2.13×10^{-7}	1.36×10^{-6}
67	*SPP1*	0.11	1.10×10^{-7}	7.17×10^{-7}
68	*BLVRB*	0.54	7.88×10^{-8}	5.26×10^{-7}
69	*CTNNB1*	0.68	4.81×10^{-8}	3.37×10^{-7}
70	*HMGB1*	0.64	3.44×10^{-9}	2.53×10^{-8}
71	*STX1A*	0.38	2.84×10^{-9}	2.14×10^{-8}
72	*SEC61A1*	0.61	1.94×10^{-9}	1.50×10^{-8}
73	*LAMB3*	0.23	5.48×10^{-10}	4.35×10^{-9}
74	*SLC20A1*	0.53	2.17×10^{-10}	1.77×10^{-9}
75	*LDHA*	0.65	6.93×10^{-11}	5.82×10^{-10}
76	*VEGFA*	0.34	5.55×10^{-11}	4.80×10^{-10}
77	*DRG1*	0.48	7.57×10^{-12}	6.74×10^{-11}
78	*TMEM255B*	0.32	6.59×10^{-12}	6.06×10^{-11}
79	*SLC7A1*	0.43	4.79×10^{-12}	4.55×10^{-11}
80	*ARL4D*	0.30	3.14×10^{-12}	3.08×10^{-11}
81	*SGK1*	0.34	2.96×10^{-13}	3.00×10^{-12}
82	*AOC2*	0.22	3.42×10^{-14}	4.02×10^{-13}
83	*CD151*	0.58	1.20×10^{-14}	1.53×10^{-13}
84	*CRLF1*	0.47	7.24×10^{-15}	9.85×10^{-14}
85	*ALDH1A2*	0.33	6.10×10^{-15}	8.96×10^{-14}
86	*FGF2*	0.46	1.19×10^{-16}	1.84×10^{-15}
87	*CD44*	0.52	8.00×10^{-17}	1.31×10^{-15}
88	*CD55*	0.36	2.13×10^{-24}	4.18×10^{-23}
89	*EMP1*	0.45	7.47×10^{-25}	1.57×10^{-23}
90	*ITGA5*	0.48	9.69×10^{-27}	2.37×10^{-25}
91	*COL6A3*	0.48	3.10×10^{-28}	8.29×10^{-27}
92	*EPAS1*	0.32	1.37×10^{-28}	4.02×10^{-27}
93	*IGFBP4*	0.20	1.53×10^{-30}	5.00×10^{-29}
94	*MKNK2*	0.24	9.85×10^{-33}	4.14×10^{-31}
95	*SERPINE1*	0.19	6.52×10^{-40}	3.84×10^{-38}

***To correct for multiple testing. the Benjamini–Hochberg method was applied to *P*-values and reported as the FDR. Gene expression changes measured in RNA sequencing data between lesioned OA articular cartilage treated with hiMSC-gel and lesioned OA articular cartilage untreated as reference. FC: fold change; FDR: false discovery rate

A